ELSEVIER

The Journal of Heart and Lung Transplantation
http://www.jhltonline.org

ORIGINAL PRE-CLINICAL SCIENCE

Extracorporeal driveline vibrations to detect left ventricular assist device thrombosis – A porcine model study

Didrik Lilja[a,b,1,2] Itai Schalit[a,3] Andreas Espinoza[a,4] Tom Nilsen Hoel[c,5] Guttorm Larsen[a,6] Fred-Johan Pettersen[d,e,7] and Per Steinar Halvorsen[a,b,8]

From the [a]The Intervention Centre, Division of Technology and Innovation, Oslo University Hospital, Oslo, Norway; [b]Institute of Clinical Medicine, University of Oslo, Oslo, Norway; [c]Department of Cardiothoracic Surgery, Oslo University Hospital, Oslo, Norway; [d]Department of Clinical and Biomedical Engineering, Oslo University Hospital, Oslo, Norway; and the [e]Department of Physics, University of Oslo, Oslo, Norway.

KEYWORDS:
LVAD pump thrombosis;
detection;
accelerometer;
driveline;
vibrations

BACKGROUND: Pump thrombosis (PT) and related adverse complications contributed to the HeartWare Ventricular Assist Device (HVAD) market withdrawal. Many patients still receive lifelong support, with deficient PT surveillance based on pump power trends. Analysis of pump vibrations is better for detecting PT. Here, we investigated the feasibility of an extracorporeal accelerometer to detect PT from pump vibrations propagated out on the driveline.

METHODS: In a porcine HVAD model (n = 6), an accelerometer was attached to the pump as a reference and another to the driveline for comparisons of signals. In total, 59 thrombi were injected into the heart to induce PT, followed by intermittent thrombus washout maneuvers. Signals were compared visually in spectrograms and quantitatively in third harmonic saliences (S_{3H}) by correlation analysis. Receiver operating characteristic curves expressed the method's outcome in sensitivity vs specificity, with the overall diagnostic performance in the area under the curve (AUC) score.

RESULTS: Five experiments had good driveline signal strength, with clear spectrographic relationships between the 2 accelerometers. Third harmonic driveline vibrations were visible 20 vs 30 times in the reference. The comparison in S_{3H} showed a strong correlation and yielded an AUC of 0.85. Notably, S_{3H} proved robust regarding noise and false PT detections.

CONCLUSIONS: An extracorporeal accelerometer on the driveline can be a readily available method for accurate HVAD PT detection before an accelerometer integration with left ventricular assist device is feasible.
J Heart Lung Transplant 2024;43:111–119

Reprint requests: Didrik Lilja, The Intervention Centre, Oslo University Hospital, Rikshospitalet, Box 4950 Nydalen, 0424, Oslo, Norway.
E-mail address: didlil@ous-hf.no.
[1] **ORCID ID:** 0000–0002-7969–1750
[2] Twitter: @didrik_lilja
[3] **ORCID ID:** 0000–0002-5411–122X
[4] **ORCID ID:** 0000–0002-6230–3088
[5] **ORCID ID:** 0000–0003-4808–9537
[6] **ORCID ID:** 0000–0003-2815–3378
[7] **ORCID ID:** 0000–0002-6359–9634
[8] **ORCID ID:** 0000–0003-3415–1184

https://doi.org/10.1016/j.healun.2023.08.022

Background

The implant of a left ventricular assist device (LVAD) is an established treatment for severe heart failure.[1–3] Due to pump thrombosis (PT), thromboembolic stroke, organ failure, and pump malfunction persist to exist as dire complications.[4–9] PT contributed to the HVAD market withdrawal in 2021, which left about 4,000 patients on HeartWare Ventricular Assist Device (HVAD) support at risk, many receiving lifelong support.[10] Neither have technological advances with the newer HeartMate 3 eliminated the risks of thrombus ingestion or formation at the inflow cannula.[4,7,9]

Early and localized PT detection is crucial for successful therapeutic interventions and stroke prevention.[11] Today's continuous PT surveillance depends on changes in pump power (P_{LVAD}), burdened by limited sensitivity.[12–14] Kaufmann et al. demonstrated that prominent third harmonic amplitudes in emitted HVAD™ sound occur when thromboembolic deposits cause impeller rotation imbalances.[11,15] However, acoustic signal quality is affected by the recording point, attenuation in surrounding tissues, and possible conditions like pleural effusion, congestion, and edema.

Sound is vibrations, which led us to use continuous pump-attached accelerometer signals to detect PT. Through in vitro and porcine model demonstrations, this utility proved superior in diagnostic capabilities to P_{LVAD}.[14,16] In addition, the accelerometer may unveil gradual inflow obstruction from elevated nonharmonic vibrations.[17–19]

It is reasonable to assume that sentinel vibrations for PT can propagate along the driveline and be detected by an accelerometer outside the body. If so, it would be of great value for existing and future patients until accelerometer integration with LVAD is feasible, as recently called for.[20] In this experimental HVAD™ in vivo study, we aimed to investigate the feasibility of accelerometer-captured driveline vibrations to diagnose PT, especially intrapump thrombosis. We hypothesized that the driveline accelerometer signals reflect vibration changes measured by a pump-attached accelerometer during thromboembolic interventions and washout procedures.

Methods

We used an established porcine ischemic heart failure model (adult noroc, 85 [82–88] kg) with HVAD (Medtronic Inc., Minneapolis, MN) support,[14,18] as shown in Figure 1A. The experiments adhered to European legislation[21] and were approved by Norwegian regulatory authorities (reference ID 19478). The 3R principle obligated us to be restrictive in animal usage.

We reused separate LVADs explanted from patients. Therefore, the drivelines had to be spliced. All the LVADs were tested before the experiments in a mock loop with 5% glucose fluid.[19] This allowed us to verify normal function, including the absence of prominent third harmonic vibrations, and check if vibrations on the drivelines echoed the pump vibrations.

General anesthesia and implantation procedures have been reported previously in detail.[14,18] Briefly, we (1) implanted HVAD with a triaxial reference accelerometer (CS1; Cardiaccs AS, Oslo, Norway) attached by median sternotomy while on cardiopulmonary bypass until LVAD startup; (2) snared the circumflex branch of the left coronary artery and set the pump speed to 2,400 rpm; and (3) inserted a cannula for thrombus injections directly into the left atrium, allowing for provoked PT by thrombus ingestion into the pump.

For this study, the driveline was tunneled through the abdominal wall approximately 15 to 25 cm from the heart. Another accelerometer, identical to the reference, was taped to the driveline as close as possible to the skin to measure propagated pump vibrations (Figure 1A). Its component axes (x, y, and z) were aligned with x along the cable direction and with y and z perpendicular to x. Before anticoagulation, whole blood (300 ml) was drawn from the animal to prepare thrombi (0.2-1.0 ml) for thromboembolic interventions.[14]

Estimates of the total cardiac output (CO) were obtained by pulmonary artery catheter (Swan-Ganz; Edwards Lifesciences, Irvine, CA) and thermodilution. An ultrasonic flowmeter system (M4; Spectrum Medical, Cheltenham, England) monitored the graft's flow rate (Q). Inclusion required Q ≥50% of the CO and stable hemodynamics verified by electrocardiogram and invasive blood pressures at the baseline before any intervention took place.

Interventions

We conducted 10 (± 1) thrombus injections by a formerly described method[14] (Figure 1B). Subsequent brief pump stops were intermittently done for thrombus material washout to induce signal changes[22] (Figure 1C).

The analysis did not include injection periods, typically lasting 30 to 60 seconds. Subsequent measurement phases were divided into acute and steady states. Based on prior experiences,[3] we let the acute phase be the immediate ≥1 minute from the injection until a steady-state phase of ≥2 minutes at the end of each intervention period. An additional ≥2-minute steady-state phase followed every pump stop.

Data acquisition

Accelerometer signals had a 375 Hz effective bandwidth, encompassing the first to ninth harmonic orders of the pump speed and were continuously and synchronously collected at a 4,000 S/s sample rate by a dedicated acquisition system.[19] Values of Q were logged separately at 1 S/s. We noted P_{LVAD} from the LVAD monitor and invasive blood pressures at the beginning of each steady-state phase.

Data processing

Processing details are presented in Supplementary Figure S1. Accelerometer signals were transformed into spectrograms. From the spectrograms, we separately extracted the third and fourth harmonic amplitudes. Then we compensated for surrounding nonharmonic amplitudes at ± 0.05 harmonic orders away from the harmonic of interest (Figure S1C). This method provided the saliences of the third harmonic (S_{3H}) and the fourth harmonic (S_{4H}). It also canceled out the effect of spikes, recognized as vertical spectrogram stripes. Using the decibel scale and the quotient rule for logarithm, S_{3H} and S_{4H} become signal-to-noise ratio analogs.

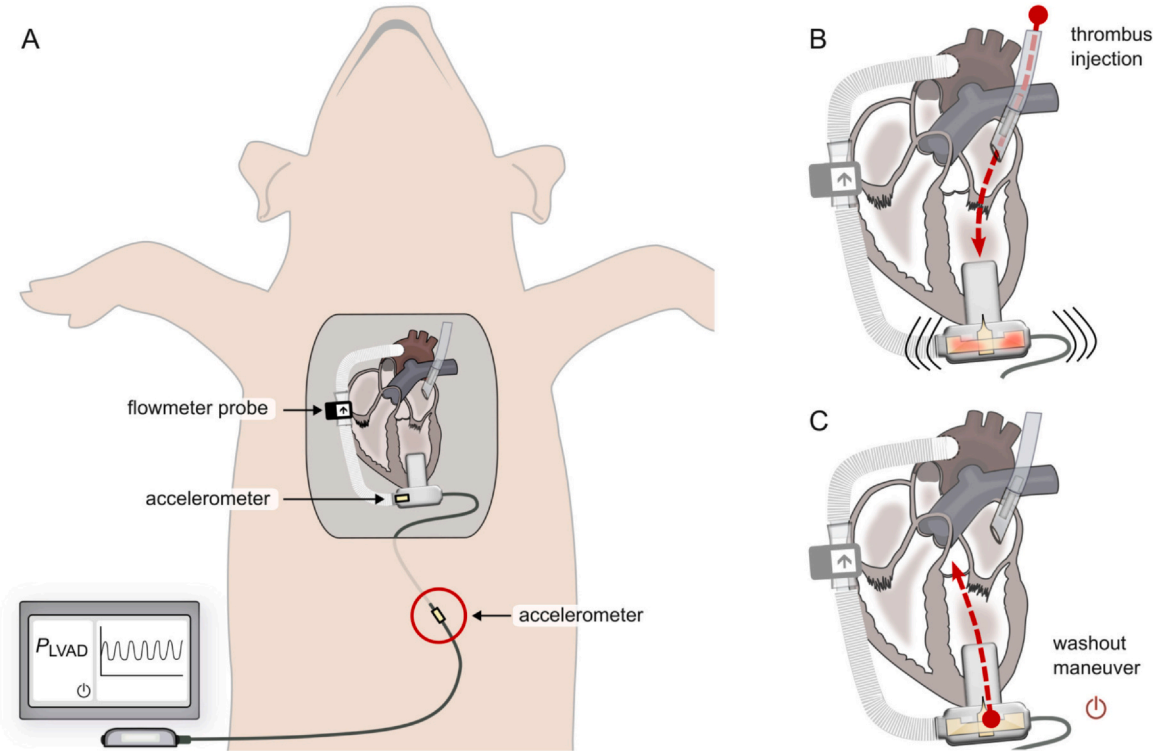

Fig. 1 Porcine HVAD model measurements and interventions. (A) Data collection; 1 reference accelerometer on the pump and another (encircled) on the driveline, outside the body, sending synchronous vibration signals to a digital acquisition system (not shown). A clip-on probe on the output graft measured the pump flow, while the pump power (P_{LVAD}) was noted from the pump monitor. (B) Intervention to provoke PT. Intrapump thrombosis is illustrated, which typically causes third harmonic pump vibrations. (C) Intervention on washout maneuver by a pump stop lasting 10 to 20 sec as an attempt to suck thrombus material from the pump and eject it into the aorta by the native heart. HVAD, HeartWare Ventricular Assist Device .

Data analysis

Amplitudes at all frequencies of accelerometer signals were qualitatively evaluated by spectrogram visualizations in the batlow colormap[23] and curve plots of S_{3H} (Figure 2). Crisp and continuous harmonic stripes verified reference signal integrity. Low nonharmonic amplitudes (primarily blue) above the second harmonic at the baseline verified an acceptable reference noise level. The absence of a visual third harmonic defined a normal pump function at baseline. Presented spectrograms have common *y* axes of where signal changes were most pronounced.

Frequential information from the driveline accelerometer was evaluated in view of the pump house accelerometer, which acted as a reference for PT.[14,16–20] For comparison, the Q and P_{LVAD} were plotted alongside. We noted the number of times the intervention caused acute discernable changes in reference accelerometer spectrograms (third harmonic or nonharmonic) as signs of ingestion. For both accelerometers, we noted how many segments where the third harmonic was visible or changed from the intervention.

Statistical method

The statistical metric was the median of S_{3H} and S_{4H} computed per measurement phase. Only the highest spatial component medians went into the analysis. The fourth harmonic is typically the most intense harmonic under normal conditions;[15] we let high values of the S_{4H} metric define good signal strength for the driveline accelerometer. Descriptive statistics are presented for the driveline S_{3H} metric, with the pump house S_{3H} metric as a reference.

First, we computed Pearson's and Spearman's correlation coefficients for S_{3H} for the 2 sensor locations per experiment. Second, reference detections of intrapump thrombosis were made by elevated pump house accelerometer S_{3H},[11,20] above a threshold calculated from baseline values as the mean + standard deviation (SD). This defined true positive for receiver operating characteristics (ROC) analysis,[24] with sensitivities plotted against specificities. The areas under the curve (AUC) score summarized the overall diagnostic performance. AUC confidence intervals were computed from bootstrapping in 1,000 iterations. To avoid false positives, the best sensitivity that pertained to 100% specificity defined the driveline S_{3H} cutoff used to calculate the negative predictive value.

Results

The study included 6 pigs. The same animals have previously been reported on with another objective to first test the detection of inflow obstructions simulated by a balloon-tip catheter and the pump-attached accelerometer.[18] For the present study, interventions commenced afterward, and the data obtained have not been published before. Table 1 presents baseline characteristics. At baseline, the graft flow was stable and 75% of the CO on average.

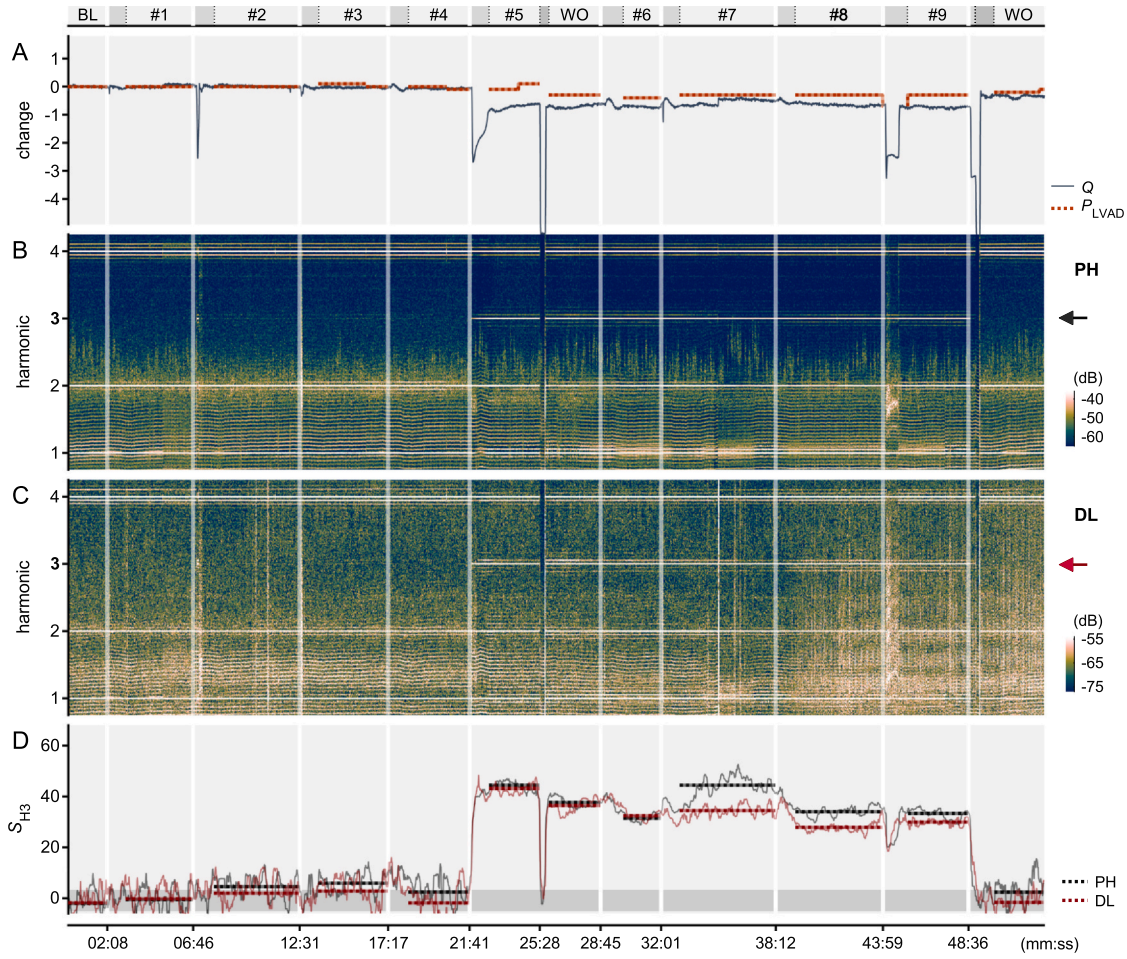

Fig. 2 Accelerometer comparison and pump reference data. The top bar indicates baseline (BL), thrombus injections (#1-9), and washout (WO) maneuvers after injections #5 and #9. (A) Pump power, P_{LVAD} (W); graft flow, Q (l/min). (B) The spectrogram of vibrations measured on the pump house (PH). To the right, the black arrow points where horizontal third harmonic stripes indicate intrapump thrombosis. (C) The spectrogram of vibrations captured by the driveline (DL) accelerometer, visualized on a shifted color scale. Like panel B, the red arrow points where third harmonic stripes indicate thrombosis. (D) Third harmonic salience ($S_{3\mathrm{H}}$) derived from the spectrograms of the pump house (gray lines) and the driveline (red lines). The thinner curves are the 20-sample moving medians, while the thicker dotted lines are the segment-wise medians used in the statistical analysis. The bottom shade marks the nonsalient range for the pump house $S_{3\mathrm{H}}$. Thick black lines above this area were regarded as proof of intrapump thrombosis for the diagnostic analysis of the driveline $S_{3\mathrm{H}}$.

We conducted 59 thrombus injections and 33 washout maneuvers after a subset of the injections (Table 2). All reported measurements are shown in Supplementary Figures S2-S7. Of the injections, 73% caused discernible acute signs of thrombus pump ingestion.

Spectrogram assessments

High-integrity accelerometer signals were obtained from the pump house accelerometer (Supplementary Figures S2-S7, panel B). Good driveline signal quality was observed in 5 of 6 experiments.

Third harmonic stripes (Figure 2) and nonharmonic patterns (Figure 3) emerged in the spectrograms after the thrombus injections, predominantly isolated from one another. Nonharmonic patterns were most pronounced between the first and fourth harmonic. Subsequent washout maneuvers usually led to the changes or disappearance of these features. Occurrences of these features in driveline spectrograms mirrored the morphology seen in the reference.

The reference accelerometer signals showed a persistent third harmonic stripe in 35 of the 92 steady-state segments. A driveline third harmonic was visible in 20 of these 35 segments. It was always accompanied by a prominent third harmonic of the pump house vibrations. Changes in the third harmonic, after either thrombus injections or washouts, occurred 27 and 17 times for the pump house and driveline, respectively. Both the third harmonic and nonharmonic patterns could be seen in the presence of noise (Figure 3).

Clear third harmonic stripes occurred in reference accelerometer signal in 5 experiments. The third harmonic was also seen in the driveline spectrograms in these experiments, except for the one with poor signals. The remaining 1 experiment had a barely visible third harmonic that did not show in the driveline spectrogram (Supplementary Figure 7B).

Table 1 Baseline Characteristics

	LVAD monitor	Flowmeter		Thermodilution		Invasive measurements			ECG
No.	P_{LVAD} (W)	Q mean (l/min)	Q SD (l/min)	CO (l/min)	Q/CO (%)	MAP (mm Hg)	MPAP (mm Hg)	CVP (mm Hg)	HR
1	2.3	2.66	0.00	3.7	72	57	28	9	116
2	2.5	2.86	0.00	4.2	68	56	26	2	106
3	2.5	3.63	0.00	6.8	53	63	22	11	125
4	2.8	4.25	0.00	4.2	101	43	27	12	72
5	2.5	3.50	0.00	3.3	106	48	28	12	76
6	2.5	3.34	0.05	6.4	52	68	16	7	75

Listed per experiment (No.): the pump power (P_{LVAD}), graft flow (Q), cardiac output (CO) by thermodilution, the Q/CO ratio, mean arterial pressure (MAP), mean pulmonary artery pressure (MPAP), central venous pressure (CVP), and the heart rate (HR).

Table 2 Summary of Third Harmonic Visibility in Vibrations Spectrograms

	Third harmonic presence		Third harmonic change	
No.	Pump house	Driveline	Pump house	Driveline
1	6	4	5	5
2	2	0	1	0
3	8	6	2	2
4	13	6	7	2
5	4	4	8	8
6	2	0	4	0
Total	35	20	27	17

Listed per experiment (No.) with the 2 accelerometer locations juxtaposed is how many steady-state segments contained an observable persistent third harmonic stripe in spectrograms and the number of times the stripe intensity appeared visually to change. The presence of a third harmonic in pump house spectrograms was our reference indication of intrapump thrombosis.

Third harmonic salience

Determined from baseline measurements, $S_{3H} = 3.3$ defined the intrapump thrombosis indication threshold in the reference signal, which corresponded with the spectrographic visibility of the third harmonic. Notably, the S_{3H} remained marginally affected by nonharmonic patterns and noise, including spikes (Figure 3C).

ROC analysis for driveline S_{3H} yielded AUC = 0.79 for the acute phases and AUC = 0.85 for the steady-state phases (Figure 4). The latter had 61% sensitivity pertained to 100% specificity and a cutoff of 2.0, which translates to a positive predictive value of 100% and a negative predictive value of 73%. There was baseline consistency and good correlation between the 2 accelerometers in 4 of the 5 experiments with good signal (Figure 5A and C-E).

Pump power

Only minor deviations in P_{LVAD} occurred throughout the experiments, within the range of −1.1 to 0.4 W and just once in magnitude > 1 W. The mean deviation was 0.1 (SD = 0.26) W.

Discussion

This in vivo study demonstrated that it is possible to diagnose PT by an extracorporeal vibration sensor on the HVAD driveline. Spectrographic vibration features reflected the directly measured vibrations on the pump house. The third harmonic salience (S_{3H}) demonstrated strong correlations between the 2 measurement locations in most experiments and good AUC. Our findings involve a readily available external method for PT surveillance before accelerometer integration on the pump is available, which could lead to better treatment outcomes by revealing subclinical PT and added reassurance for the patients at a low cost and practically no risks.

The injection-related appearances of third harmonic stripes or nonharmonic spectrographic patterns in the reference spectrograms are clinically relevant. Respectively, such features concur with related studies involving provoked intrapump thrombosis[14,16] and inflow obstructions.[17–19] All these studies demonstrated a superior diagnostic capability of a pump-attached accelerometer over changes in pointwise logged P_{LVAD}, the routine clinical method. Others have reported corroborative findings for this from acoustic analysis.[12,15,25] In this study, P_{LVAD} provided practically no PT indications.[11,26,27] It was deficient even by tighter detection thresholds used in refined power-based algorithms.[28,29] When the graft flow was reduced, concurrent friction might have counteracted a drop in P_{LVAD}.[11] Smaller thrombus deposits might not have caused flow reduction nor filled the impeller-housing gap and created friction but adhered to the impeller and caused third harmonic vibrations. Continuous pump power waveforms can supply valuable information,[27,30] but it remains challenging to account for a complex and extensive individual variation. Instead, until an accelerometer integration with LVAD is in place, we demonstrated the possibility of getting reliable PT indications outside the body.

The averaged CO portion through the LVAD agreed well with the 73% of injections that imprinted signs of ingestion in the reference spectrograms. Therefore, the ability of the reference method to indicate acutely provoked PT is substantiated.

Our focus was on third harmonic driveline vibrations to detect intrapump thrombosis. The third harmonic stripes

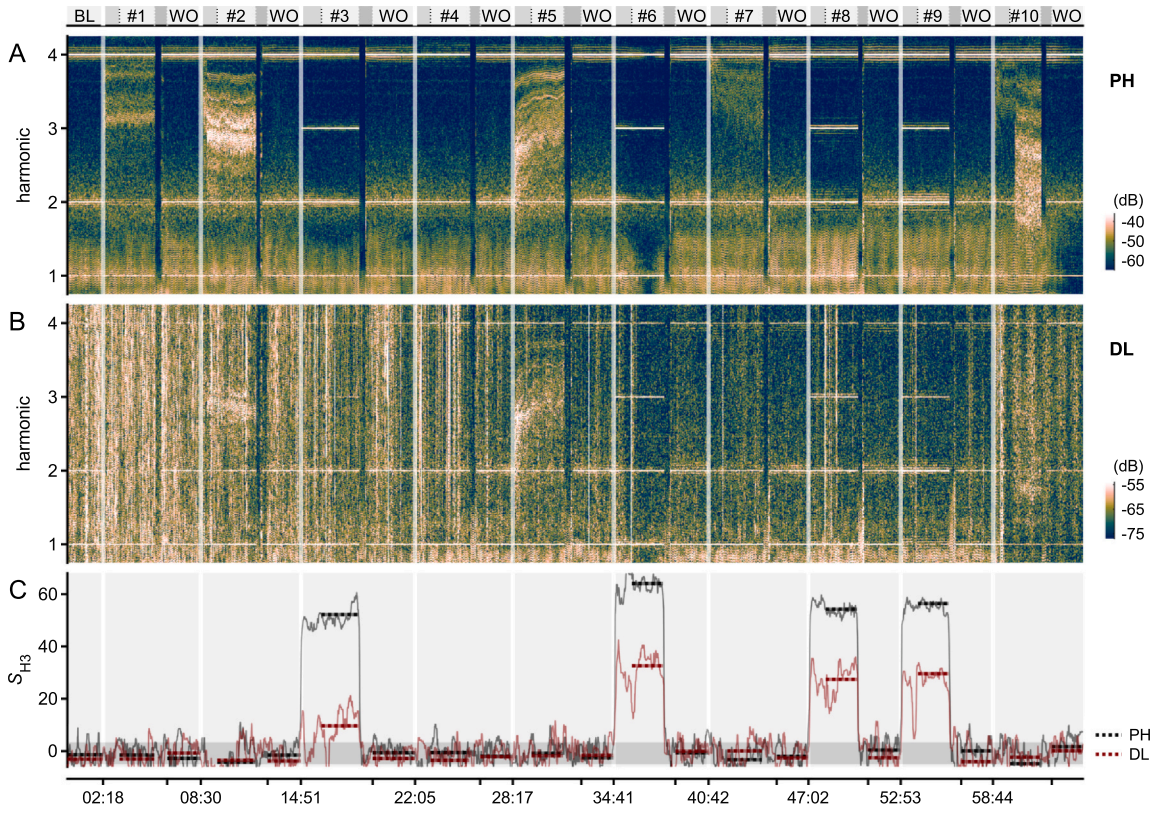

Fig. 3 Elaborate example with driveline third harmonic robustness against noise. The top bar indicates baseline (BL) and thrombus injections (#1-10) alternatingly done with washout (WO) maneuvers. (A) The pump house (PH) accelerometer spectrogram with intermittent third harmonic stripes at #3, #6, #8, and #9, indicative of intrapump thrombosis. Substantial nonharmonic patterns occurred after injections #1, #2, #5, #7, and #10, preferentially due to thromboembolism in the inflow cannula. (B) The corresponding spectrogram by the driveline (DL) accelerometer. The color scale is shifted to gain suitable contrast for propagated pump vibrations but also amplifies the noise and spike-related spontaneous vertical stripes. (C) Derived third harmonic salience (S_{3H}) for both accelerometers overlaid. The thinner and thicker lines are the moving and segment-wise medians, respectively.

and S_{3H} curves (Figures S2-S7C and D) and S_{3H} medians (Figure 5) convey a compelling reflection of the reference accelerometer in 4 of 6 experiments. Of note, the washout maneuvers often reduced the third harmonic vibrations at both accelerometer locations. Yet, a persistent third harmonic could indicate incomplete washouts or thrombolytic therapy (after injection #3, Figure S5). Another finding is that driveline S_{3H} never elevated without a concomitant presence in the reference.

Two experiments had no driveline S_{3H} elevation. Of them, the weak signal experiment had only 1 reference occurrence of S_{3H} elevation. An exclusion of it would hardly alter the ROC AUC. The other experiment (Figure S7) had sufficient driveline signal strength to reflect the nonharmonic pattern after injection #6 but not for the subtle third harmonic stripes in the reference signals. This does not oppose the otherwise good covariation observed and the encouraging results obtained through ROC analysis (Figure 4).

Noise, including plentiful spikes of unknown origin, had little influence on how the S_{3H} curves from the 2 locations covaried (Figure 3). The S_{3H} definition ensured robustness against spikes, whereas the median-based time aggregation attenuated scattered noise. Moreover, the nonharmonic patterns often penetrated through the noise. As such, a good spectrographic impression relies on the color scale, but that is irrelevant for S_{3H}. Anyhow, a time-domain spike filtering would be advisable for quantifying nonharmonic amplitudes.[1,2] Another idea is to investigate if additional accelerometers can enhance the signal-to-noise ratio or if rotational movements captured by a gyroscope can be exploited as supplementary information. Furthermore, the spectrographic contrast to nonpulsatile in vitro studies[16,19] suggests cardiac motion as slightly wavy horizontal stripes. These occurred below the second harmonic for all support levels in Table 1, leaving S_{3H} and S_{4H} unaffected.

Nonharmonic vibrations often occurred isolated before the third harmonic elevated. The washout maneuver always made a gainful effect in clearing out nonharmonic patterns, for example, as seen in Figure 3, as one may anticipate for inflow cannula thromboembolism.[17–19] Lone nonharmonic patterns in the acute phase, as by injection 9 in Figure 2, could signify a passing embolus while crumbled by the impeller. Detection of such events may warn for possible residuals deposited in the pump and inducement of PT formation.[16,31,32]

The close spectrographic relationship between the 2 accelerometer signals shows that the vibrations are transmitted along the driveline, although the abdominal wall tissue may dampen and disperse the vibrations. Dampening

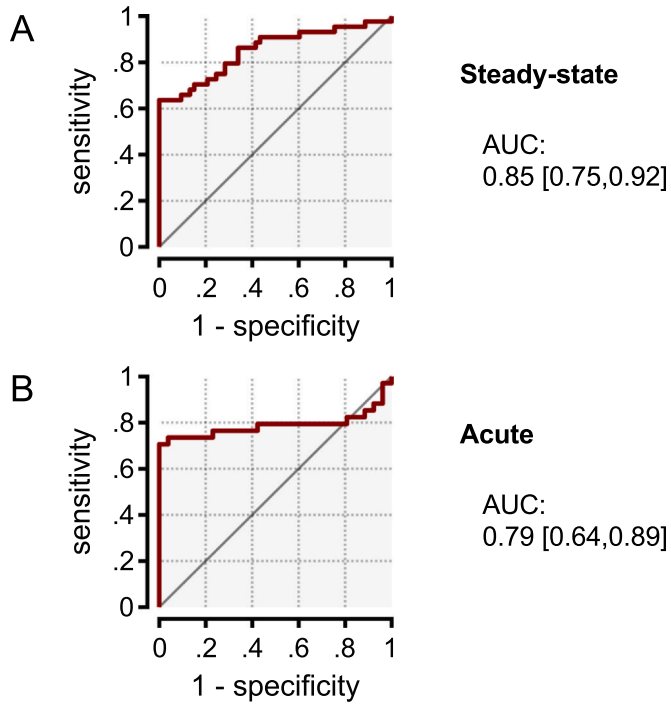

Fig. 4 Diagnostic performances of driveline vibration monitoring for intrapump thrombosis using ROC analysis. (A) Performance regarding the immediate acute phase. (B) Performance regarding the steady-state phase. The curves are based on spectrogram saliences of accelerometer-captured third harmonic vibration (S_{3H}) and different cutoff values for detection, with the pump-attached accelerometer as reference. For the overall diagnostic performance, areas under the curve (AUC) are given with confidence intervals in brackets.

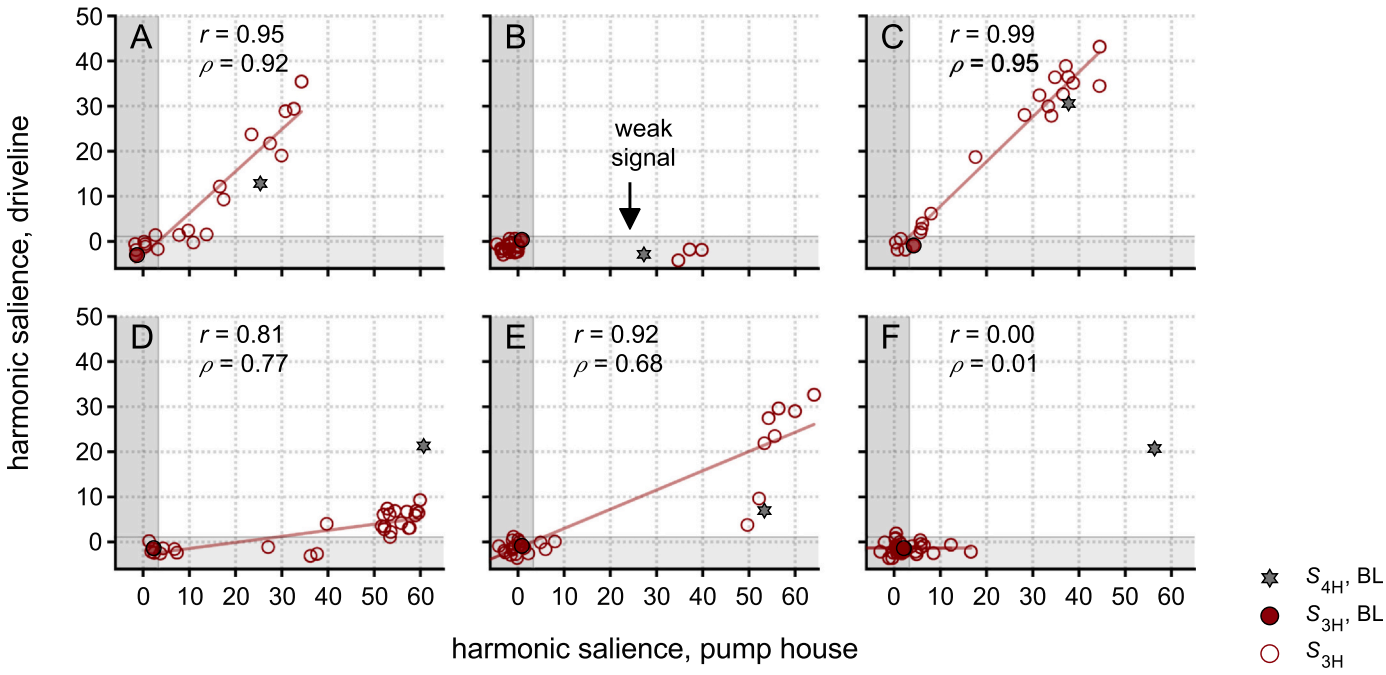

Fig. 5 Harmonic salience comparisons. Per experiment, in the separate panels A to F, segment-wise medians of third harmonic salience (S_{3H}) are plotted in red for the pump house vs the driveline accelerometer. Values of S_{3H} are plotted in filled circles for baseline (BL) and open circles for the acute and steady-state phases after an intervention. Pearson's correlation coefficient (r) and Spearman's correlation coefficient (ρ) are correspondingly shown. The gray shades represent the nonsalient harmonic signal regions, whereas unshaded areas are true positive detections of intrapump thrombosis made by the driveline accelerometer. As a signal strength reference, the baseline fourth harmonic salience (S_{4H}) is plotted in gray hexagrams. Note that in panel B, this reference signifies unreliable signal strength, and r and the linear fit are thus omitted.

of pump vibration by a closed-chest scenario is proposedly marginal since the third harmonic is already an established acoustic sign of clinical intrapump thrombosis.[11,15]

Whether or not intrapump thrombosis leads to prominent third harmonic vibrations in other LVADs, such as the HeartMate 3, remains unknown.[33] But it is reasonable to believe that the HeartMate 3 impeller design will produce harmonic changes of some kind due to PT, perhaps better recognized using a broader bandwidth. Also, emerged nonharmonic patterns are suggested to be rather universally tied to mass pendulation within the inflow cannula.[17–19] Yet, pump vibrations might not propagate the same way on another driveline type. The abovementioned points impose the need for further research. On that note, an accelerometer retrofit solution for patient monitoring may open a "big data perspective" of even greater value and diminish the need for animal experiments.

To avoid signal interference, we envision self-served check-ups once or more a day while lying or sitting still. Continuously windowed S_{3H} medians over longer timespans can improve the detection performance regarding the signal-to-noise ratio but at the cost of sensitivity for short-term events of embolic material passing the pump. We suggest adequate fourth harmonic signal as a surveillance criterion. Why 1 experiment had poor signal quality could be explained by a loose driveline splice that hindered the propagation of vibrations. For the 3 experiments with the weakest signals, the splices might have also modulated the driveline vibrations into the 2 blurred horizontal stripes at harmonic orders of 1.3 and 2.5, regarded as artifacts (Figures S3, S5, and S7, panel B). If so, these issues would not happen with an original driveline.

Limitations

It is unknown to what extent the signal strength was influenced by the distance from the pump to the accelerometer placement from the varying driveline length inside the pericardium. Therefore, the expected presence of fourth harmonic driveline vibration needs real-world validation.

The protocol did not include other pump speeds than 2,400 rpm, whereas the global clinical average is 2,645 rpm,[27] but increased speed tended to amplify vibrations of PT in previous studies.[18,19] Nor was the Lavare speed modulation enabled.[21] Speed modulation could cause spikes originating in jerks exerted on the driveline but regularly per minute and can thus be ignored in the signal processing. Another concern for HeartMate 3 support is the frequent speed variation to create an artificial pulse and possible vortex-related noise.[34] This may obscure nonharmonic patterns of thromboembolism but not S_{3H} because of the shown noise and spike robustness.

The study is exploratory. The AUC confidence bands signified statistical significance of the method, although from serial intervention in few experiments. Verification and establishing clinical cutoff values warrant patient population study.

Conclusion

An extracorporeal accelerometer on the driveline can sense pump vibrations indicative of PT. Indications from third harmonic driveline vibrations had a compelling diagnostic capability, referenced against directly measured pump vibrations. Our findings may have valuable implications in the diagnostics of PT, allowing therapeutic interventions before PT becomes overt. HVAD driveline monitorization for PT can be swiftly implemented until accelerometer integration on the pump is realized, a concept that may as well apply to the HeartMate 3.

Author contributions

Didrik Lilja: Conceptualization, methodology, software, formal analysis, investigation, data curation, writing – original draft, writing – review & editing, resources, visualization, and project administration; **Itai Schalit**: Conceptualization, methodology, investigation, and data curation, writing – original draft, writing – review & editing and resources; **Andreas Espinoza**: Conceptualization, methodology, investigation, data curation, resources, writing – original draft, writing – review & editing and supervision; **Tom Nilsen Hoel**: Methodology and investigation; **Fred-Johan Pettersen**: Methodology, writing – original draft, writing – review & editing and supervision; **Guttorm Larsen**: Methodology, investigation, resources, and data curation; **Per Steinar Halvorsen**: Conceptualization, methodology, investigation, resources, data curation, writing – original draft, writing – review & editing, supervision, project administration, and funding acquisition.

Disclosure statement

P.S.H.and A.E. are shareholders in the company Cardiaccs AS, which possesses a pending patent on the concept of using implanted accelerometers to monitor LVADs. We report no other financial conflict of interest.

Acknowledgments

The study was funded by the South-Eastern Norway Regional Health Authority (grant ID 2018016).

Anne Marie Marstein made a considerable contribution to experiment logistics. The same did Helen Littorin-Sandbu, besides giving anesthesia. Arnt Eltvedt Fiane, from the Department of Cardiothoracic Surgery, did an excellent job as the operator in several experiments and with project administration.

Appendix A. Supporting information

Supplementary data associated with this article can be found in the online version at doi:10.1016/j.healun.2023.08.022.

References

1. Gustafsson F, Rogers JG. Left ventricular assist device therapy in advanced heart failure: patient selection and outcomes. Eur J Heart Fail 2017;19(5):595-602.
2. Pinney SP, Anyanwu AC, Lala A, Teuteberg JJ, Uriel N, Mehra MR. Left ventricular assist devices for lifelong support. J Am Coll Cardiol 2017;69(23):2845-61.
3. Molina EJ, Shah P, Kiernan MS, et al. The Society of Thoracic Surgeons Intermacs 2020 Annual Report. Ann Thorac Surg 2021;111(3):778-92.
4. Netuka I, Mehra MR. Ischemic stroke and subsequent thrombosis within a HeartMate 3 left ventricular assist system: a cautionary tale. J Heart Lung Transplant 2018;37(1):170-2.
5. Najjar SS, Slaughter MS, Pagani FD, et al. An analysis of pump thrombus events in patients in the HeartWare ADVANCE bridge to transplant and continued access protocol trial. J Heart Lung Transplant 2014;33(1):23-34.
6. Neidlin M, Liao S, Li Z, et al. Understanding the influence of left ventricular assist device inflow cannula alignment and the risk of intraventricular thrombosis. Biomed Eng OnLine 2021;20(1):20-47.
7. Eulert-Grehn J-J, Krabatsch T, Potapov E. A case of an obstructive inflow thrombus in a HeartMate 3 from the left ventricle into the pump. J Heart Lung Transplant 2018;37(1):172-3.
8. Mehra MR, Uriel N, Naka Y, et al. A fully magnetically levitated left ventricular assist device — Final report. N Engl J Med 2019;380(17):1618-27.
9. Chiang YP, Cox D, Schroder JN, et al. Stroke risk following implantation of current generation centrifugal flow left ventricular assist devices. J Cardiac Surg 2020;35(2):383-9.
10. Tops LF, Coats AJS, Ben Gal T. The ever-changing field of mechanical circulatory support: new challenges at the advent of the 'single device era'. Eur J Heart Fail 2021;23(9):1428-31.
11. Scandroglio AM, Kaufmann F, Pieri M, et al. Diagnosis and treatment algorithm for blood flow obstructions in patients with left ventricular assist device. J Am Coll Cardiol 2016;67(23):2758-68.
12. Semiz B, Hersek S, Pouyan MB, et al. Detecting suspected pump thrombosis in left ventricular assist devices via acoustic analysis. IEEE J Biomed Health Inform 2020;24(7):1899-906.
13. Pappalardo F, Bertoldi LF, Sanvito F, Marini C, Consolo F. Inflow cannula obstruction of the HeartWare left ventricular assist device: what do we really know? Cardiovasc Pathol 2021;50:107299.
14. Schalit I, Espinoza A, Pettersen FJ, et al. Detection of thromboembolic events and pump thrombosis in HeartWare HVAD using accelerometer in a porcine model. ASAIO J 2020;66(1):38-48.
15. Kaufmann F, Hörmandinger C, Stepanenko A, et al. Acoustic spectral analysis for determining pump thrombosis in rotary blood pumps. ASAIO J 2014;60(5):502-7.
16. Schalit I, Espinoza A, Pettersen FJ, et al. Accelerometer detects pump thrombosis and thromboembolic events in an in vitro HVAD circuit. ASAIO J 2018;64(5):601-9.
17. Schalit I, Espinoza A, Pettersen F-J, et al. Improved detection of thromboembolic complications in left ventricular assist device by novel accelerometer-based analysis. ASAIO J 2022;68(9):1117-25.
18. Lilja D, Schalit I, Espinoza A, et al. Detection of inflow obstruction in left ventricular assist devices by accelerometer: a porcine model study. J Heart Lung Transplant 2023;42(8):1005-14.
19. Lilja D, Schalit I, Espinoza A, Pettersen F-J, Elle OJ, Halvorsen PS. Detection of inflow obstruction in left ventricular assist devices by accelerometer: an in vitro study. Med Eng Phys 2022;110:103917.
20. Antaki JF. A lone vibration crying in the wilderness. ASAIO J 2022;68:9.
21 Directive 2010/63/EU of 22 September 2010 on the protection of animals used for scientific purposes. 2010.[accessed March 1, 2023]. Available from: https://eur-lex.europa.eu/LexUriServ/LexUriServ.do?uri=OJ:L:2010:276:0033:0079:en:PDF.
22. Potapov EV, Krabatsch T, Buz S, Falk V, Kempfert J. Cerebral protection system applied during washout of thrombus occluding inflow cannula of HeartWare HVAD left ventricular assist device. J Heart Lung Transplant 2015;34(12):1640-1.
23. Crameri F, Shephard GE, Heron PJ. The misuse of colour in science communication. Nat Commun 2020;11:1.
24. Zou KH, O'Malley AJ, Mauri L. Receiver-operating characteristic analysis for evaluating diagnostic tests and predictive models. Circulation 2007;115(5):654-7.
25. Feldmann C, Deniz E, Stomps A, et al. An acoustic method for systematic ventricular assist device thrombus evaluation with a novel artificial thrombus model. J Thorac Dis 2018;10(S15):S1711-9.
26. Goldstein DJ, John R, Salerno C, et al. Algorithm for the diagnosis and management of suspected pump thrombus. J Heart Lung Transplant 2013;32(7):667-70.
27. Hayward C, Adachi I, Baudart S, et al. Global best practices consensus: long-term management of patients with hybrid centrifugal flow left ventricular assist device support. J Thorac Cardiovasc Surg 2022;164(4):1120-37. e2.
28. Slaughter MS, Schlöglhofer T, Rich JD, et al. A power tracking algorithm for early detection of centrifugal flow pump thrombosis. ASAIO J 2021;67(9):1018-25.
29. Grabska J, Schlöglhofer T, Gross C, et al. Early detection of pump thrombosis in patients with left ventricular assist device. ASAIO J 2019;66(4).
30. Rich JD, Burkhoff D. HVAD flow waveform morphologies: theoretical foundation and implications for clinical practice. ASAIO J 2017;63(5):526-35.
31. Rowlands GW, Antaki JF. High-speed visualization of ingested, ejected, adherent, and disintegrated thrombus in contemporary ventricular assist devices. Artif Organs 2020;44(11):E459-69.
32. Jessen SL, Kaulfus CN, Chorpenning K, Ginn-Hedman A-M, Tamez D, Weeks BR. Histologic features of thrombosis events with a centrifugal left ventricular assist device. J Heart Lung Transplant 2021;40(1):56-64.
33. Sundbom P, Roth M, Granfeldt H, et al. Sound analysis of the magnetically levitated left ventricular assist device HeartMate 3™. Int J Artif Organs 2019;42(12):717-24.
34. Wiegmann L, Thamsen B, de Zélicourt D, et al. Fluid dynamics in the HeartMate 3: influence of the artificial pulse feature and residual cardiac pulsation. Artif Organs 2019;43(4):363-76.